

A Coral-Like Mo₂C/TiO₂ Photoelectrode for Photoelectrochemical Water Splitting (Fotoelektrod Mo₂C/TiO₂ Berstruktur Karang untuk Aplikasi Pembelahan Air Fotoelektrokimia)

SITI NURUL FALAEIN MORIDON¹, KHUZAIMAH ARIFIN^{1,3,*}, LORNA JEFFERY MINGGU¹, MOHAMAD AZUWA MOHAMED², MASLIANA MUSLIMIN⁴, AHMAD ZAKI ZAINI² & MOHAMMAD B. KASSIM^{1,2}

¹*Fuel Cell Institute, Universiti Kebangsaan Malaysia, 43600 UKM Bangi, Selangor, Malaysia*

²*Department of Chemical Sciences, Faculty of Science and Technology, Universiti Kebangsaan Malaysia, 43600 UKM Bangi, Selangor, Malaysia*

³*Research Center for Advanced Materials, National Research and Innovation Agency (BRIN), Tangerang Selatan 15314, Indonesia*

⁴*Agensi Nuklear Malaysia, 43000 Kajang, Bangi, Selangor, Malaysia*

Received: 21 June 2023/Accepted: 4 December 2023

ABSTRACT

Titanium dioxide (TiO₂) is one of the most explored photoelectrode materials of water splitting for hydrogen generation. However, TiO₂ has a bandgap of 3.2 eV, which restricts its energy absorption to UV light, and the photoexcited electrons and holes swiftly recombine. Thus, alteration of the band structure, such as by adding materials as cocatalysts, is needed. 2D molybdenum carbide (Mo₂C) has been researched extensively as an excellent non-noble cocatalyst owing to its Pt-like H⁺ adsorption capacity and high conductivity. In this work, composites of TiO₂ and Mo₂C with four different compositions were produced using the sol-gel method, and their photoelectrochemical activity for water splitting was assessed. The composites were spin-coated onto FTO conducting glass, and FESEM analysis indicated that TiO₂ nanoparticles are widely disseminated across Mo₂C to form coral-like structures. Analysis via X-ray diffraction verified the existence of peaks composed of TiO₂ and Mo₂C. The sample containing 3% Mo₂C had the greatest increase in photocurrent density, which was approximately 1.56 mA cm⁻² at a potential of 1.0 V against Ag/AgCl (1.59 vs. RHE), which is five times that of bare TiO₂. In addition, the composite's onset potential moved to a lower potential. Our findings suggest that adding Mo₂C increases the photoelectrochemical performance of the TiO₂ photoelectrode. This work indicates the feasibility of employing Mo₂C as a cocatalyst to improve the performance of TiO₂ for photoelectrochemical H₂ production.

Keywords: Molybdenum carbide (Mo₂C); photoanode and water-splitting; titanium dioxide (TiO₂)

ABSTRAK

Titanium dioksida (TiO₂) merupakan salah satu bahan fotoelektrod yang paling diterokai untuk aplikasi pembelahan molekul air bagi penjanaan gas hidrogen. Namun, TiO₂ mempunyai jurang jalur lebar 3.2 eV yang mengehadkan penyerapan tenaganya kepada cahaya UV serta elektron dan lohong foto teruja bergabung semula dengan cepat. Oleh itu, pengubahan struktur jalur dengan kaedah seperti penambahan bahan tambah sebagai ko-pemangkin amat diperlukan. Molibdenum karbida 2D (Mo₂C) telah dikaji secara meluas sebagai ko-pemangkin kerana kapasiti penyerapan H⁺ seperti Pt dan kekonduksian yang tinggi. Dalam kajian ini, komposit TiO₂ dan Mo₂C dengan empat komposisi berbeza dihasilkan menggunakan kaedah sol-gel dan aktiviti fotoelektrokimia bagi proses pembelahan air dinilai. Komposit ini disapukan pada kaca konduktif FTO melalui kaedah salutan putaran dan analisis FESEM menunjukkan bahawa nanozarah TiO₂ tersebar luas di sekitar Mo₂C untuk membentuk struktur seperti karang. Analisis melalui difraksi sinar-X mengesahkan kewujudan puncak yang terdiri daripada TiO₂ dan Mo₂C. Sampel yang mengandungi 3% Mo₂C menunjukkan peningkatan ketumpatan fotoarus yang terbesar, iaitu sekitar 1.56 mA cm⁻² pada keupayaan 1.0 V berbanding dengan Ag/AgCl (1.59 berbanding RHE), yang merupakan lima kali ganda TiO₂ kosong. Selain itu, keupayaan permulaan komposit bergerak ke keupayaan yang lebih rendah. Penemuan kami menunjukkan bahawa penambahan Mo₂C meningkatkan prestasi fotoelektrokimia fotoelektrod TiO₂. Kajian ini menunjukkan kerealisan penggunaan Mo₂C sebagai ko-pemangkin untuk meningkatkan prestasi TiO₂ dalam penghasilan H₂ secara fotoelektrokimia.

Kata kunci: Fotoarus dan pembelahan air; molibdenum karbida (Mo₂C); titanium dioksida (TiO₂)

INTRODUCTION

Fossil fuels, which currently dominate the energy sector, are facing depletion and environmental issues. The utilization of fossil fuels is a major contributor to carbon emissions, which cause climate change. To address these issues, we need to diversify our energy resources by incorporating renewable and sustainable sources while also accelerating the adoption of low or zero-net carbon technologies like a fuel cell system. Hydrogen, an abundant element on Earth, is a promising energy carrier that can be used as fuel for a fuel cell system to generate electricity. These hydrogen fuel cells are known as clean and safe technology, with the byproduct being only pure water, which also significantly contributes to reducing carbon emissions (Moridon et al. 2022a). However, hydrogen is rarely found in the form of hydrogen gas on Earth. It often binds with other elements to form hydrocarbons, water, acids, or base molecules. We need to extract hydrogen from these sources. Among the methods of hydrogen production, photoelectrochemical (PEC) water splitting, which utilizes sunlight energy, offers a source of green hydrogen. This method has the potential to be more cost-effective, as it can use low-cost semiconductor materials and be implemented in a compact, single-system design (Ng et al. 2018).

Titanium dioxide (TiO_2) was the first material used in photoelectrochemical (PEC) water splitting to produce H_2 and O_2 (Mustafid Amna et al. 2020). TiO_2 remains a subject of extensive study due to its effectiveness, stability, and affordability in liquid environments (Moridon et al. 2022b). However, unaltered TiO_2 exhibits low efficiency in H_2 production due to charge recombination and high overpotential (Khuzaimah et al. 2021; Moridon et al. 2022a). To address these challenges, researchers have explored various solutions, including the addition of cocatalysts to enhance oxidation or reduction reactions and the creation of heterojunctions to facilitate efficient transport and promote spatial charge separation. Among cocatalysts, platinum (Pt) nanoparticles (NPs) have shown great promise for TiO_2 , but their cost remains a concern.

Currently, transition metal carbides, like molybdenum carbide (Mo_2C), show potential as low-cost alternatives to platinum (Liu et al. 2021; Seh et al. 2016). Mo_2C enhances TiO_2 catalytic activity in various reactions. However, the effectiveness depends on Mo_2C loading. This study investigates the optimal Mo_2C weight percentage on TiO_2 for efficient PEC water splitting. We synthesized $\text{Mo}_2\text{C}/\text{TiO}_2$ photocatalysts with different

Mo_2C amounts via the sol-gel process to analyze their photocatalytic activity.

MATERIALS AND METHODS

MATERIALS

TiO_2 Degussa (99%; obtained from Merck), molybdenum carbide (Mo_2C) (99%; obtained from Sigma Aldrich), ethanol (analytical grade; obtained from QReC), polyethylene glycol (PEG) (99%; obtained from Sigma Aldrich), deionized water and sodium sulfate (Na_2SO_4) were used. All chemicals were used as received from the manufacturer without additional purification.

PREPARATION OF $\text{Mo}_2\text{C}/\text{TiO}_2$ NP COMPOSITE

To produce a 1 wt% $\text{Mo}_2\text{C}/\text{TiO}_2$ ratio sample, we measured 0.2 g of commercialized TiO_2 and 0.02 g of Mo_2C , following the method outlined by Yue et al. (2017). Next, the measured sample was mixed with a solution containing 30 mL of ethanol and 20 mL of polyethylene glycol (PEG), and the mixture was stirred using a magnetic stirrer for 30 min. Afterward, we spin-coated the resulting mixture onto the FTO substrate at 1000 revolutions per minute. We repeated a similar procedure for other concentrations of Mo_2C : 2%, 3%, and 4% by weight.

PHOTOELECTROCHEMICAL ANALYSIS

The PEC analysis was conducted utilizing the Ametek Versastat 4, a widely recognized and commonly employed instrument in the field. In the photoelectrochemical cell experiment, a working electrode with an exposed area of 1 cm^2 was utilized. The counter electrode was comprised of a platinum wire, while an Ag/AgCl electrode was employed as the reference electrode to quantify the potential difference across the two electrodes. The experiments were conducted using an electrolyte solution containing 0.5 M Na_2SO_4 , which exhibited a pH value of 6.7. The current density on the surfaces of the thin film was assessed under two conditions: in the absence of light (dark) and under solar AM 1.5 illumination. The illumination was achieved by employing a xenon lamp (Oriel) with an intensity of 100 mW cm^{-2} . The experimental technique employed in this study was linear sweep voltammetry (LSV), which involved sweeping the potential from 0 to +1.0 V relative to the Ag/AgCl reference electrode. The electrolyte used was a 0.5 M Na_2SO_4 solution, and the scan rate employed

was 5 mV s^{-1} . In order to acquire a more comprehensive comprehension of the charge transport characteristics demonstrated by the photoanodes that were synthesized, a Mott-Schottky analysis was conducted at a frequency of 1 kHz. Equation (1) can be used to compute electron density based on the slope of the of the Mott-Schottky plots.

$$Nd = 2/d \left(\frac{1}{C^2} \right) / e \epsilon \epsilon_0 \left(\frac{1}{dV} \right) \quad (1)$$

where Nd is donor density; e is electron charge; ϵ denotes dielectric constant of sample; ϵ_0 is permittivity of vacuum; and V is the applied potential at electrode surface. We also used electrochemical impedance spectroscopy (EIS) to analyze interface resistance. EIS Nyquist plots were constructed using 10 mV sinusoidal perturbations at frequencies of 100 kHz, with a voltage of 0.7 V versus Ag/AgCl applied.

CHARACTERIZATION

The process of collecting of X-ray diffraction (XRD) patterns was performed using a Bruker D-8 Advance instrument. X-ray photoelectron spectroscopy (XPS) was conducted utilising a Kratos/Shimadzu instrument, specifically the Axis Ultra DLD model. The primary objective of this analysis was to ascertain the chemical phase that exists within the crystalline substance under investigation. The X-ray diffraction (XRD) spectra were subjected to analysis utilising the Xpert high-score software. In order to examine the topography of the surface, we conducted field emission scanning electron microscopy (FESEM) using a Zeiss Merlin Compact microscope. The optical properties of the sample were examined utilising a Perkin Elmer ultraviolet/visible/near-infrared spectrophotometer (UV-VIS-NIR) with the specific model being Lambda 950.

RESULTS AND DISCUSSION

PHOTOELECTROCHEMICAL AND ELECTRICAL PROPERTIES

In this study, the weight percentage of Mo_2C varied from 1 wt% to 4 wt% to determine the optimal weight percentage for maximal photocatalytic activity. Figure 1(a) displays the photocurrent of TiO_2 , Mo_2C , and TiO_2 loaded with 1 wt% to 4 wt% Mo_2C . Among the various weight percentages, TiO_2 loaded with 3 wt% Mo_2C exhibited the highest photocurrent, reaching nearly 1.56

mA cm^{-2} at 1 V vs. Ag/AgCl (equivalent to 1.59 vs. RHE). This performance surpassed that of other weight percentages. Comparing the results to a previous study by Yue et al. (2017), it was observed that, at zero bias, 1 wt% Mo_2C loaded onto TiO_2 was capable of achieving $1.8 \mu\text{A cm}^{-2}$. In our study, this value increased substantially, nearly 500 times, reaching 0.5 mA cm^{-2} at zero bias. The significant improvement in photocurrent density can be attributed to the presence of Mo_2C , which acts as an electron sink, preventing electrons emitted from the conduction band of TiO_2 from recombining with holes (Yue et al. 2017). The optimal Mo_2C concentration appears to 3 wt%, while higher Mo_2C loading can lead to particle aggregation and reduced surface area, while lower loading may not provide sufficient sites for efficient charge transfer (Li et al. 2013; Yue et al. 2017). Further, the analysis focuses on a sample of 3% $\text{Mo}_2\text{C}/\text{TiO}_2$. Electrochemical impedance spectroscopy (EIS) is an effective method for analyzing interface resistance. In this study, a voltage of 0.7 V vs. Ag/AgCl is applied to the sample of 3% $\text{Mo}_2\text{C}/\text{TiO}_2$ and compared with pure TiO_2 as shown on a Nyquist plot in Figure 1(b). The semicircle arc of sample 3% $\text{Mo}_2\text{C}/\text{TiO}_2$ was found lower than sample of pure TiO_2 , indicating enhanced electrical conductivity and lower resistance. This is in line with the photocurrent density results, where the presence of Mo_2C promotes electron transfer between TiO_2 particles and reduces electron-hole recombination.

To assess the photostability of the material, chopping chronoamperometry was employed. In this study, we varied the voltages 0 V, 0.2 V, and 0.4 V to measure the photostability of 3 wt% $\text{Mo}_2\text{C}/\text{TiO}_2$ over a period of 900 s. As shown in Figure 1(c), at 0 V, the photocurrent density remained relatively stable until around 500 s into the process, and only slight decrease, until 900 s photocatalytic duration. Furthermore, when an applied voltage of 0.2 V was introduced, the photocurrent density increased by approximately 30% compared to the initial 0 V, and then after 200 s, the photocurrent gradually decreased with value approach photocurrent produced at 0 V. And this photocurrent density produced maintain until 900 s. A significant improvement in photocurrent density was observed at 0.4 V at the early stages of the illumination process. The photocurrent density gradually reduced and stabilized after 700 s, maintaining at $\sim 1.4 \text{ mA cm}^{-2}$ until the end of the 900 s process. However, when the voltage was increased to 0.5 V, the chronoamperometric measurements could not be detected. This suggests the possibility of material

degradation or damage at higher voltages, leading to a decrease in photocurrent or loss of activity. A previous study has proposed the theory that at high voltages, the material may undergo electrochemical reactions such as oxidation or reduction, resulting in the formation of new chemical species. Nonetheless, these new chemical species might not be discernible using the chopped chronoamperometry approach (Wang et al. 2017).

Additionally, Mott-Schottky analysis is a standard electrochemical method for elucidating the conductivity type and carrier density of semiconducting materials. The Mott-Schottky analysis of pure TiO_2 and 3 wt% $\text{Mo}_2\text{C}/\text{TiO}_2$ samples shown in Figure 1(d), where both samples shows positive slopes indicating n-type semiconductors. A n-type semiconductor will possess as photoanode. The photoanode flat band potential (V_{FB}) values were calculated by extrapolating the x-intercepts of the linear area in the Mott-Schottky plots using

Equation (1). TiO_2 and 3 wt% $\text{Mo}_2\text{C}/\text{TiO}_2$ photoanodes were all found to have different VFB values relative to Ag/AgCl , with -0.66 V and -0.41 V , respectively. The donor density (ND) of the materials may also be determined by the slope of the Mott-Schottky curves and Equation (3). The value of the ND is shown in Table 1. A semiconductor material with a high donor density has a significant number of donor impurities or atoms, which results in a greater concentration of free electrons in the conduction band. Higher slopes are generally associated with lower flatband potentials and higher donor densities, which are both ideal characteristics for a semiconductor photoelectrode (Hankin et al. 2019). This improves the material's electrical conductivity and accelerates electron transport. Hence, Mott-Schottky analysis is helpful in understanding the electrical characteristics of photoanodes and their viability as photocatalysts.

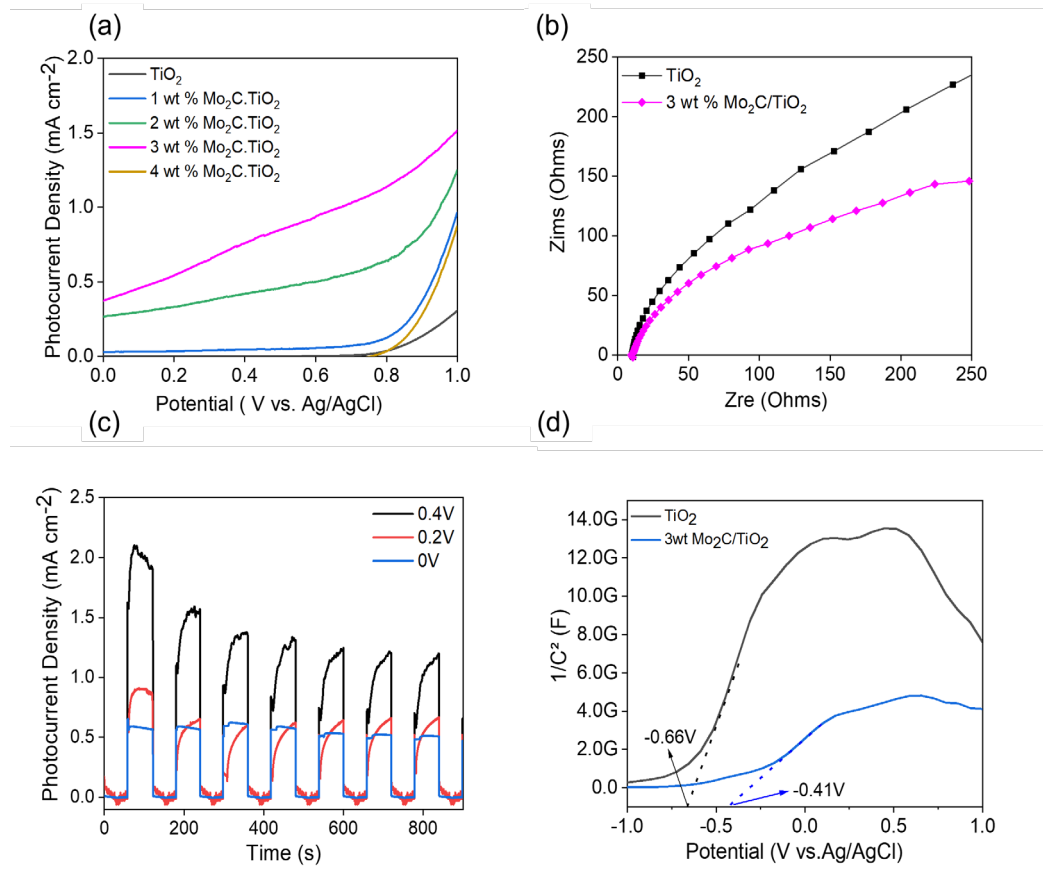


FIGURE 1. (a) Photocurrent density, (b) EIS analysis (c) chronoamperometry of 3 wt% of $\text{Mo}_2\text{C}/\text{TiO}_2$, (d) Mott-Schottky of TiO_2 , and 3 wt% of $\text{Mo}_2\text{C}/\text{TiO}_2$

OPTICAL PROPERTIES

To verify the role of Mo_2C as a cocatalyst, the photocatalyst's optical properties with diffuse reflectance spectroscopy was carried out. Figure 2(a) is spectrum absorption of pure TiO_2 and 3 wt% $\text{Mo}_2\text{C}/\text{TiO}_2$ samples, in which pure TiO_2 , tends to absorb more UV than visible light. Meanwhile, 3 wt% $\text{Mo}_2\text{C}/\text{TiO}_2$ sample absorb visible light slightly higher than pure TiO_2 . It is widely assumed that introducing Mo_2C into TiO_2 might generate local states above the valence band edge, resulting in band-gap narrowing. As shown in Figure 2(b), the band gap value of 3 wt% $\text{Mo}_2\text{C}/\text{TiO}_2$ was determined to be 3.05 eV, which was lower than that of pure TiO_2 (3.16 eV) and proved that the existence of Mo_2C caused the band gap to decrease. The value of the band gap of TiO_2 is 2.89 eV. The value of E_{VB} is calculated using the Mulliken

electronegativity theory according to Equations (2) and (3) (Praus 2021):

$$E_{\text{VB}} = X - E_e + 0.5 * E_{\text{gap}} \quad (2)$$

$$E_{\text{CB}} = E_{\text{VB}} - E_{\text{gap}} \quad (3)$$

The energies of the conduction band (CB) and valence band (VB) of a semiconductor are relative to the normal hydrogen electrode (NHE) and represented by E_{CB} and E_{VB} , respectively. The electronegativity (TiO_2 has an X value of 5.81) (Zhou et al. 2019), band gap (E_{g}), and energy of free electrons ($E_e = 4.5$ eV) of the semiconductor also play a role in determining these bands.

TABLE 1. Flat band potential (E_{fb}) and donor density (N_{D}) of TiO_2 , Mo_2C and 3 wt% $\text{Mo}_2\text{C}/\text{TiO}_2$

Semiconductor	N_{D}	E_{FB} (V)
TiO_2	2.69×10^{33}	-0.66
3wt% $\text{Mo}_2\text{C}/\text{TiO}_2$	4.62×10^{36}	-0.41

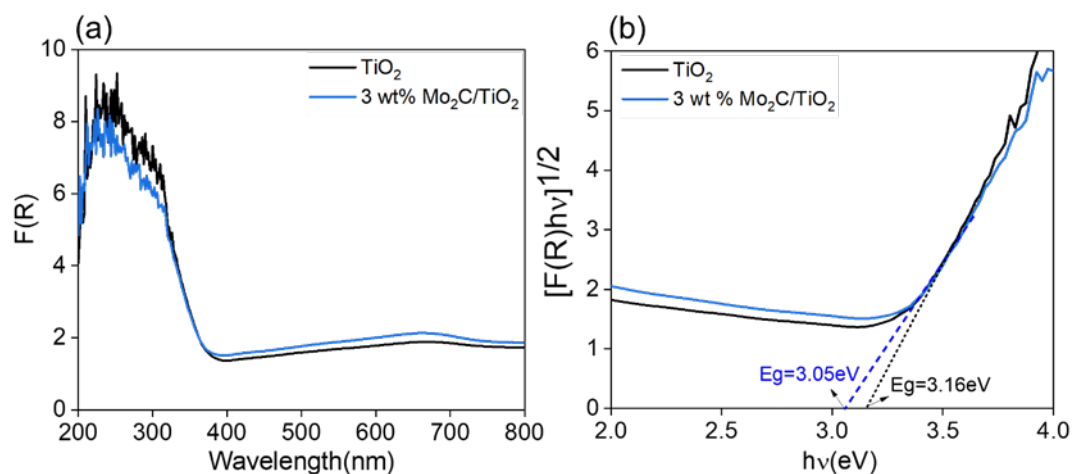


FIGURE 2. (a) Absorbance data Kubelka-Munk curves and (b) band gap determination Tauc plots

The combination of Mo_2C with TiO_2 in photoelectrochemical water splitting applications serves as a cocatalyst that can significantly improve the overall photoelectrochemical performance of the TiO_2 photoelectrode. The presence of Mo_2C in the composite material can modify the band structure of TiO_2 , reducing its band gap and broadening the range of light absorption. This allows the electrode to harvest more of the solar spectrum and generate more photoexcited charge carriers. Overall, the addition of Mo_2C to TiO_2 in photoelectrochemical water-splitting applications serves as a powerful strategy for improving the photoelectrochemical performance of the electrode and enhancing the efficiency of the water splitting reaction.

The measurement of applied bias photon-to-current efficiency (ABPE) serves as a crucial parameter in evaluating the efficacy of a photoelectrochemical cell in its conversion of solar energy into practical electrical energy. Furthermore, this technique proves to be valuable in the assessment of different materials' efficacy in the conversion of light energy into electrical energy, as well as in the evaluation of the performance of individual components. Figure 3 shows the ABPE measurement of TiO_2 and 3 wt% $\text{Mo}_2\text{C}/\text{TiO}_2$. The ABPE value was calculated using the following Equation (3):

$$\text{ABPE \%} = [J_p (E_0 \text{ rev} - E_{\text{app}}) / I_0] * 100 \quad (3)$$

In the given equation, J_p represents the photocurrent density (measured in mA/cm^2), I_0 denotes the illumination intensity (measured in mW/cm^2), $E_0 \text{ rev}$ signifies the standard reversible potential for water splitting (1.23 V), and E_{app} represents the applied potential. The maximum anodic photocurrent bias enhancement (APBE) value observed for TiO_2 is 10% at an applied voltage of 0.8 V. In contrast, the APBE value for 3 wt% $\text{Mo}_2\text{C}/\text{TiO}_2$ reaches 55% at 0 V. This result demonstrates that the inclusion of Mo_2C enhances the photocatalytic performance of the TiO_2 photoanode while simultaneously reducing the required applied bias energy.

PHASE AND MORPHOLOGICAL CHARACTERIZATIONS

X-ray diffraction (XRD) analysis is an incredibly powerful method for determining the crystallographic structure of materials. Figure 4 shows the XRD patterns for TiO_2 , Mo_2C and 3 wt% $\text{Mo}_2\text{C}/\text{TiO}_2$ samples. TiO_2 anatase phases 25.32° (011), 37.73° (013), 47.90° (020), 54.57° (121) and 65.44° (024) are detected, along with Mo_2C phases 34.38° (010), 39.38° (021), and 75.29° (011) (Li et al. 2013). The analysis showed that TiO_2 and 3 wt% $\text{Mo}_2\text{C}/\text{TiO}_2$ samples displayed some variations in their peaks at 20° to $30^\circ 2\theta$. The shift toward the left can be attributed to several factors, such as modifications in the lattice parameters or a reduction in the size of the crystallites. The presence of Mo_2C in the 3 wt% $\text{Mo}_2\text{C}/\text{TiO}_2$ sample was confirmed by the appearance of a small

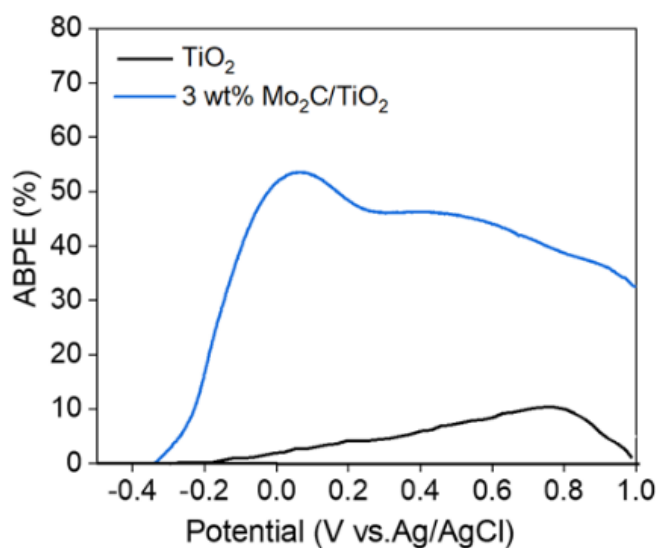


FIGURE 3. ABPE of TiO_2 and 3 wt% $\text{Mo}_2\text{C}/\text{TiO}_2$

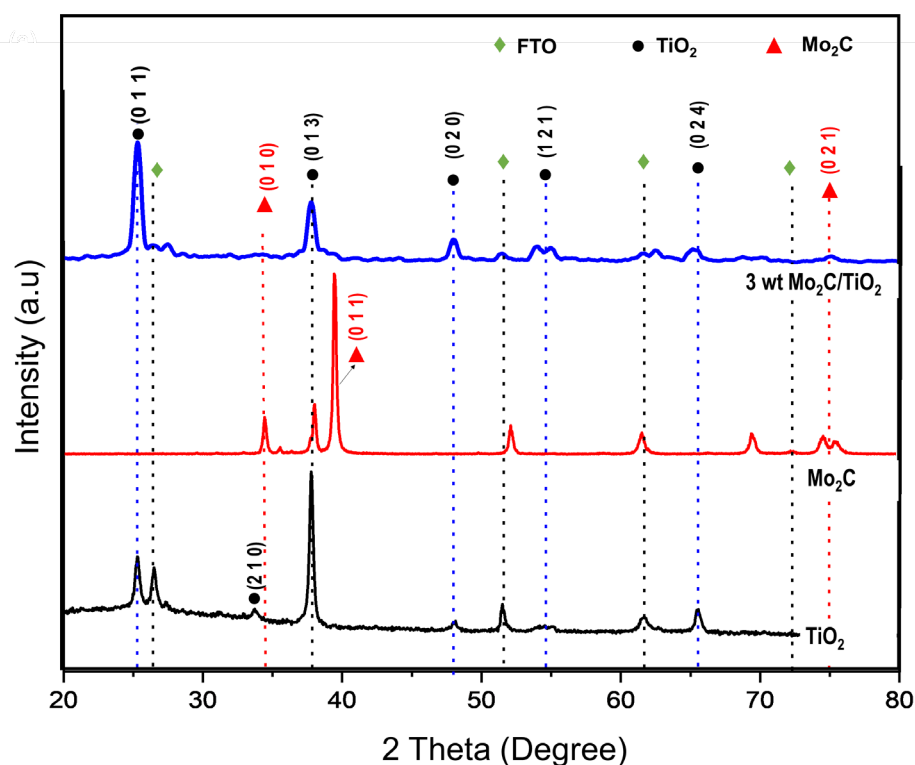


FIGURE 4. XRD spectra of Mo_2C , TiO_2 , and 3 wt% $\text{Mo}_2\text{C}/\text{TiO}_2$ 20-80°

peak at 75°, corresponding to Mo_2C . The peak's intensity is relatively low due to the Mo_2C content being only around 3%. The merging of two peaks may be due to an overlapping of different crystallographic planes within the same crystal structure. This can occur when the lattice parameters of the crystal are slightly distorted or when there are defects or imperfections in the crystal lattice.

The following method, known as X-ray photoelectron spectroscopy (XPS), is employed to analyze the chemical composition of a material's surface by measuring the energy of photoelectrons emitted when the surface is exposed to X-rays. Figure 5 displays high-resolution (HR) spectra for Ti 2p, Mo 3d, and O 1s, along with their corresponding fitted peaks, for pure TiO_2 , Mo_2C and 3 wt% $\text{Mo}_2\text{C}/\text{TiO}_2$ samples. Figure 5(a) shows the XPS spectrum of the Ti 2p core level for TiO_2 . The two main peaks at 454.95 eV and 460.79 eV correspond to the Ti 2p^{3/2} and Ti 2p^{1/2} spin-orbit split doublet, respectively. These peaks correspond to, characteristic of Ti^{4+} that confirming the main valence state of +4 for Ti in the TiO_2 lattice. While, 459.52 eV, correspond to Ti^{3+} . Figure 5(b) shows the XPS spectrum

of the Ti 2p core level for 3wt% $\text{Mo}_2\text{C}/\text{TiO}_2$. The two main peaks are shifted to lower binding energies at 455.28 eV, 460.58 eV and 461.38 eV, respectively. This shift is due to the electron-donating effect of the Mo_2C nanoparticles. Next, Figure 5(c) shows the XPS spectrum of the O 1s core level for TiO_2 . The main peak at 527.96 eV is attributed to lattice oxygen Ti-O bonds in TiO_2 . A second peak at 526.26 eV is attributed to surface hydroxyl groups (OH-) Ti-OH bonds. Figure 5(d) shows the XPS spectrum of the O 1s core level for 3wt% $\text{Mo}_2\text{C}/\text{TiO}_2$. The main peak Ti-OH bonds is shifted to a lower binding energy at 527.75 eV. This shift is also due to the electron-donating effect of the Mo_2C nanoparticles. Additionally, the Ti-OH bonds peak at 526.65 eV is reduced in intensity, which suggests that the Mo_2C nanoparticles are covering some of the TiO_2 surface. Next, Figure 5(e) shows the XPS spectrum of the Mo 3d core level for Mo_2C . The two main peaks at 229.39 eV and 232.54 eV correspond to the Mo 3d^{5/2} and Mo 3d^{3/2} spin-orbit split doublet, respectively. These peaks are characteristic of Mo^{6+} in the Mo_2C structure. Figure 5(f) shows the XPS spectrum of the Mo 3d core level

for 3wt% Mo₂C/TiO₂. The two main peaks are shifted to lower binding energies at 229.27 eV and 232.4 eV, respectively. This shift is due to the electron-donating effect of the TiO₂ support. In general, the shift of a peak to the right in XPS spectra indicates an increase in the binding energy of the electrons, while a shift to the left indicates a decrease in the binding energy. As mentioned in a previous study by Mohamed et al. (2019), the shift of Ti 2p peaks to the right and Mo 3d peaks to the left can be understood in terms of changes in the electron density surrounding these atoms, with the Ti atoms

experiencing a decrease in electron density and the Mo atoms experiencing an increase in electron density due to the adsorption of CO and other species on the Mo₂C surface (Yue et al. 2017).

Overall, the XPS data shows that the Mo₂C nanoparticles are successfully deposited on the TiO₂ support. The electron-donating effect of the Mo₂C nanoparticles shifts the binding energies of the Ti 2p and O 1s core levels to lower values. Additionally, the Mo₂C nanoparticles cover some of the TiO₂ surface, which reduces the intensity of the peak at 526.0 eV in the O 1s core level spectrum.

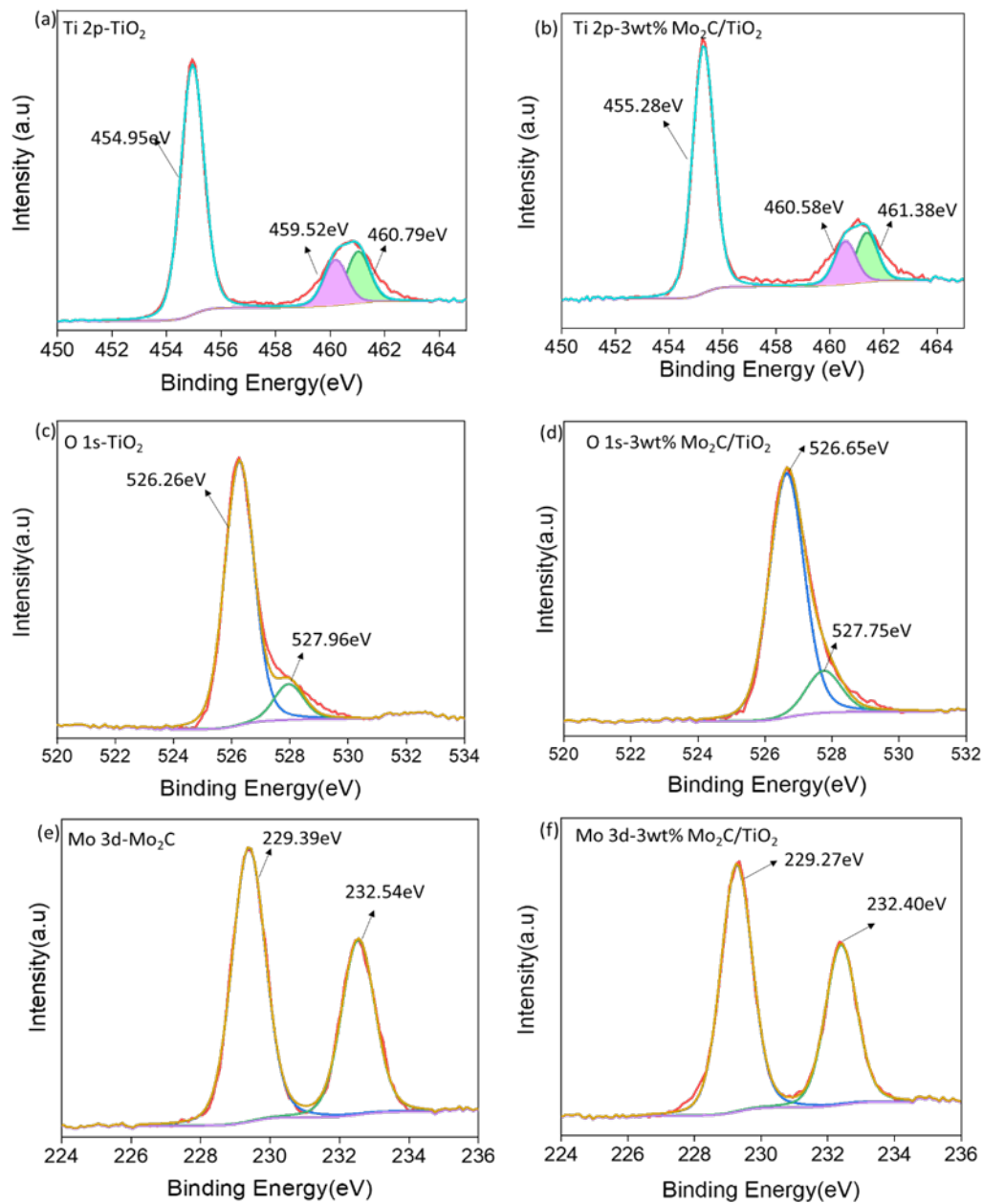


FIGURE 5. XPS analysis of Ti 2p, O 1s and Mo 3d in TiO₂, Mo₂C and 3 wt% Mo₂C/TiO₂ NP

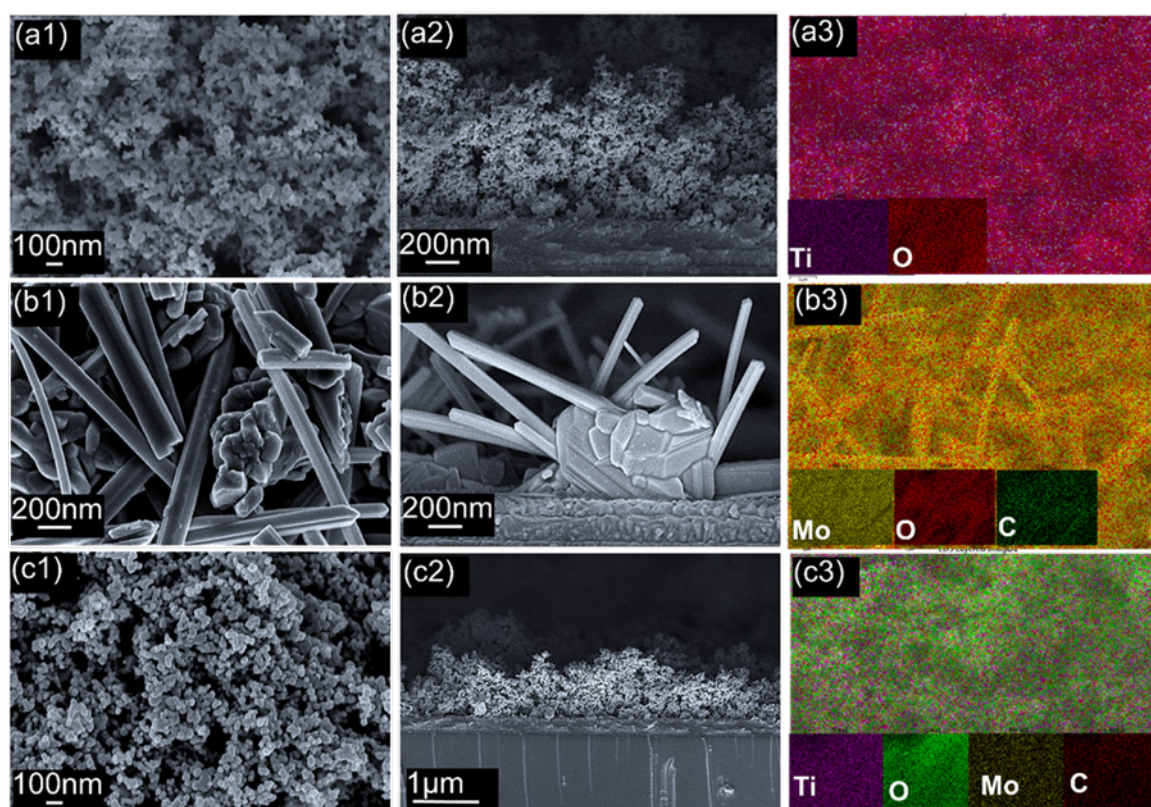


FIGURE 6. Surface image, cross section and EDX mapping of (a) TiO_2 , (b) Mo_2C and (c) 3 wt% $\text{Mo}_2\text{C}/\text{TiO}_2$

The size, shape, distribution, crystal structure, chemical content, and surface characteristics of particles evaluated by FESEM analysis. Figure 6 shows the structure and morphology of the prepared samples: TiO_2 , Mo_2C and 3 wt% $\text{Mo}_2\text{C}/\text{TiO}_2$. As shown in Figure 6(a), the FESEM image of TiO_2 shows nanoparticles with an average diameter of 60.11 nm. TiO_2 nanoparticles used for PEC water splitting typically show a uniform distribution of spherical or elongated particles with a relatively narrow size distribution, typically in the range of 10-100 nanometers, as shown in a previous study by Moridon et al. (2022b) and other works reporting the morphology of TiO_2 NPs. In regard to photocatalysis, the size of the TiO_2 nanoparticles plays a crucial role. The photoelectrochemical activity of nanoparticles may be improved by increasing their surface area, and surface imperfections can increase the rate at which photogenerated charge carriers recombine. Nevertheless, the photoelectrochemical activity may be diminished because larger nanoparticles have a smaller surface

area and fewer surface imperfections (Habibi, Foruzin & Nasirpour 2023). Meanwhile, Figure 6(b) shows the FESEM image for the Mo_2C sample; the morphology observed is a mixture of long nanorods and short clumped rods that most likely act as the seed for Mo_2C growth. Figure 6(b)(ii) shows the nanorod shape of Mo_2C with an average calculated length of 1.584 μm . According to Li et al. (2013), Mo_2C tends to form elongated nanostructures or particles with a hexagonal crystal structure (Seh et al. 2016). FESEM images of Mo_2C samples typically show a network of interconnected nanostructures, with individual particles or clusters ranging in size from tens to hundreds of nanometers. Following this, loading 3 weight percent of Mo_2C onto TiO_2 demonstrated that the Mo_2C nanorods were covered by the TiO_2 NPs, as shown in Figure 6(c). The overall morphology of the 3 wt% $\text{Mo}_2\text{C}/\text{TiO}_2$ formed a coral-like structure under FESEM analysis. Furthermore, the existence of Mo_2C can also be proven by the EDX spectrum data, as shown in Figure 6(c), which is compatible with the presence

of molybdenum, titanium, oxygen, and a small amount of carbon in the sample. This strongly shows that the Mo₂C composite heterojunction was introduced into the sample.

CONCLUSION

The utilisation of Mo₂C on TiO₂ in photoelectrochemical systems holds significant promise, as evidenced by the compelling findings of our study. The remarkable enhancement in photocurrent serves as a clear manifestation of the synergistic impact exhibited by these materials. The significant increase in photocurrent observed in this study highlights the tremendous potential of utilising the 3 wt% Mo₂C-TiO₂ combination to improve the efficiency of photoelectrochemical systems. The observed photocurrent density exhibited a substantial enhancement of approximately 5-fold, culminating in a noteworthy value of 1.56 mA cm⁻² at a potential of 1.0 V against Ag/AgCl (1.59 vs. RHE). The Mo₂C plays a crucial role in the photoelectrochemical water splitting process, exerting a substantial influence on both the Hydrogen Evolution Reaction (HER) and Oxygen Evolution Reaction (OER). This influence stems from Mo₂C's ability to generate surface electrons, which subsequently interact with H⁺ ions, leading to the production of H₂ gas. Additionally, these surface electrons also interact with O²⁻ ions, resulting in the evolution of O₂ gas. This conclusion highlights the significant potential of Mo₂C-TiO₂ in transforming solar energy conversion technologies and propelling the development of sustainable and environmentally friendly energy solutions.

ACKNOWLEDGEMENTS

This research was made possible thanks to funding from the FRGS/1/2019/STG01/UKM/03/2 that was provided by the Ministry of Education, Malaysia and Universiti Kebangsaan Malaysia for GUP-2022-078.

REFERENCES

- Habibi-Hagh, F., Foruzin, L.J. & Nasirpour, F. 2023. Remarkable improvement of photoelectrochemical water splitting in pristine and black anodic TiO₂ nanotubes by enhancing microstructural ordering and uniformity. *International Journal of Hydrogen Energy* 48(30): 11225-11236. <https://doi.org/10.1016/j.ijhydene.2022.07.158>
- Hankin, A., Bedoya-Lora, F.E., Alexander, J.C., Regoutz, A. & Kelsall, G.H. 2019. Flat band potential determination: Avoiding the pitfalls. *Journal of Materials Chemistry A* 7(45): 26162-26176. <https://doi.org/10.1039/C9TA09569A>
- Khuzaimah Arifin, Rozan Mohamad Yunus, Lorna Jeffery Minggu & Mohammad B. Kassim. 2021. Improvement of TiO₂ nanotubes for photoelectrochemical water splitting. *International Journal of Hydrogen Energy* 46(7): 4998-5024. <https://doi.org/10.1016/j.ijhydene.2020.11.063>
- Li, H., Hong, W., Cui, Y., Fan, S. & Zhu, L. 2013. Effect of Mo₂C content on the structure and photocatalytic property of Mo₂C/TiO₂ catalysts. *Journal of Alloys and Compounds* 569: 45-51. <https://doi.org/10.1016/j.jallcom.2013.03.165>
- Liu, J., Hodes, G., Yan, J. & Liu, S. (F). 2021. Metal-doped Mo₂C (metal= Fe, Co, Ni, Cu) as catalysts on TiO₂ for photocatalytic hydrogen evolution in neutral solution. *Chinese Journal of Catalysis* 42(1): 205-216.
- Mohamed, M.A., Zain, M.F.M., Minggu, L.J., Kassim, M.B., Jaafar, J., Amin, N.A.S., Mastuli, M.S., Wu, H., Wong, R.J. & Ng, Y.H. 2019. Bio-inspired hierarchical hetero-architectures of in-situ C-doped g-C₃N₄ grafted on C, N co-doped ZnO micro-flowers with booming solar photocatalytic activity. *Journal of Industrial and Engineering Chemistry* 77: 393-407. <https://doi.org/10.1016/j.jiec.2019.05.003>
- Moridon, S.N.F., Anggraini, D., Arifin, K., Minggu, L.J. & Kassim, M.B. 2022a. Photocatalytic hydrogen generation from water by TiO₂/Co₃O₄ composite photocatalysis. *Malaysian Journal of Analytical Sciences* 26(3): 581-588.
- Moridon, S.N.F., Arifin, K., Yunus, R.M., Minggu, L.J. & Kassim, M.B. 2022b. Photocatalytic water splitting performance of TiO₂ sensitized by metal chalcogenides: A review. *Ceramics International* 48(5): 5892-5907. <https://doi.org/10.1016/j.ceramint.2021.11.199>
- Mustafid Amna Rambey, Khuzaimah Arifin, Lorna Jeffery Minggu & Mohammad B. Kassim. 2020. Cobalt sulfide as photoelectrode of photoelectrochemical hydrogen generation from water. *Sains Malaysiana* 49(12): 3117-3123. <http://dx.doi.org/10.17576/jsm-2020-4912>
- Ng Kim Hang, Lorna Jeffery Minggu, Wun Fui Mark-Lee, Khuzaimah Arifin, Mohammad Hafizuddin Hj Jumali & Mohammad B. Kassim. 2018. A new method for the fabrication of a bilayer WO₃/Fe₂O₃ photoelectrode for enhanced photoelectrochemical performance. *Materials Research Bulletin* 98: 47-52. <https://doi.org/10.1016/j.materresbull.2017.04.019>
- Praus, P. 2021. On electronegativity of graphitic carbon nitride. *Carbon* 172: 729-732. <https://doi.org/10.1016/j.carbon.2020.10.074>

- Seh, Z.W., Fredrickson, K.D., Anasori, B., Kibsgaard, J., Strickler, A.L., Lukatskaya, M.R., Gogotsi, Y., Jaramillo, T.F. & Vojvodic, A. 2016. Two-dimensional molybdenum carbide (MXene) as an efficient electrocatalyst for hydrogen evolution. *ACS Energy Letters* 1(3): 589-594. <https://doi.org/10.1021/acseenergylett.6b00247>
- Wang, Q., He, J., Shi, Y., Zhang, S., Niu, T., She, H. & Bi, Y. 2017. Designing non-noble/semiconductor Bi/BiVO₄ photoelectrode for the enhanced photoelectrochemical performance. *Chemical Engineering Journal* 326: 411-418. <https://doi.org/10.1016/j.cej.2017.05.171>
- Yue, X., Yi, S., Wang, R., Zhang, Z. & Qiu, S. 2017. A novel architecture of dandelion-like Mo₂C/TiO₂ heterojunction photocatalysts towards high-performance photocatalytic hydrogen production from water splitting. *Journal of Materials Chemistry A* 5(21): 10591-10598. <https://doi.org/10.1039/C7TA02655B>
- Zhou, Y., Tan, Y., Xiang, Y. & Zhu, J. 2019. Construction of urchin-like ZnO/TiO₂ direct Z-scheme system to improve charge separation. *ChemistrySelect* 4(44): 12963-12970. <https://doi.org/10.1002/slct.201903905>

*Corresponding author; email: khuzaim@ukm.edu.my